Journal of Maps

ISSN: (Print) (Online) Journal homepage: https://www.tandfonline.com/loi/tjom20

Geology of the Imdr Regio area of Venus

Iván López, Lucía Martín, Piero D'Incecco, Nicholas P. Lang & Gaetano Di Achille

To cite this article: Iván López, Lucía Martín, Piero D'Incecco, Nicholas P. Lang & Gaetano Di Achille (2023) Geology of the Imdr Regio area of Venus, Journal of Maps, 19:1, 2253832, DOI: 10.1080/17445647.2023.2253832

To link to this article: https://doi.org/10.1080/17445647.2023.2253832

JOURNAL OF MAPS
2023, VOL. 19, NO. 1, 2253832
https://doi.org/10.1080/17445647.2023.2253832

Geology of the Imdr Regio area of Venus

Iván López[a], Lucía Martín[b], Piero D'Incecco[c,d], Nicholas P. Lang[e] and Gaetano Di Achille[c]

[a]Tecvolrisk Research Group, Departamento de Biología, Geología, Física y Química Inorgánica, Universidad Rey Juan Carlos, Madrid, Spain; [b]Volcanology Research Group, Department of Life and Earth Sciences, Instituto de Productos Naturales y Agrobiología, Consejo Superior de Investigaciones Científicas (IPNA-CSIC), Santa Cruz de Tenerife, Spain; [c]National Institute for Astrophysics (INAF), Astronomical Observatory of Abruzzo, Teramo, Italy; [d]Arctic Planetary Science Institute, Rovaniemi, Finland; [e]Department of Biochemistry, Chemistry, Geology, and Physics, Mercyhurst University, Erie, PA, USA

ABSTRACT

We present a 1:5,000,000 geological map of the Imdr Regio area of Venus. Geological mapping was conducted using synthetic aperture radar (SAR) images, altimetry and stereo-derived topography data from NASA's Magellan mission. The map covers an area of approximately 7.9×106 km2 and exhibits a variety of tectonic structures and units of volcanic origin related to the evolution of Imdr Regio and surrounding plains. We have differentiated primary structures related to the emplacement of the different units from tectonic structures that deform them. These structures are also organized between those that are regional in extent and those that are related to the evolution of local large tectono-volcanic structures. The units in the map area represent different geologic processes (e.g. volcanism) that took place during the evolution of the large topographic rise. Geologic mapping illustrates a complex evolution with different styles of deformation and volcanism in this part of the planet.

ARTICLE HISTORY
Received 30 June 2023
Revised 22 August 2023
Accepted 24 August 2023

KEYWORDS
Venus; planetary geology; Imdr regio; large topographic rises

1. Introduction

The NASA's Magellan mission obtained a near-global coverage with synthetic aperture radar (SAR) images of the surface of Venus between 1990 and 1994, revolutionizing the knowledge of our sister terrestrial planet. Data returned from the Magellan spacecraft have revealed that the surface of Venus is dominated by volcanism (e.g. Head et al., 1992) and is also characterized by an extensive tectonic activity (e.g. Solomon et al., 1992), yet the distribution of volcanism and tectonic activity suggests there is not a current system of moving plates such as those operating on Earth (Phillips & Hansen, 1994; Solomon et al., 1992). Vital to understand the geodynamic evolution of Venus and the current geologic state of the planet is the study of Large Topographic Rises (LTR), geological provinces on Venus thought to be formed in response to the presence of a mantle plume or mantle upwelling (Smrekar et al., 1997; Stofan et al., 1995), and therefore may be comparable to hot spot locations and intraplate volcanism on Earth. They are sites where the existence of recent or even active volcanism on Venus has been proposed (e.g. Herrick & Hensley, 2023; Smrekar et al., 2010), a situation that makes these areas strategic targets for future missions (D'Incecco et al., 2021).

The first step to study the geology and evolution of LTR is to constrain the structures, materials and processes that have given shape to its surface, for which the elaboration of geologic maps has proven to be a fundamental tool. Geologic mapping at a regional scale allows synthesis of the current knowledge of a studied area, and to identify existing problems to be studied with upcoming missions and their associated datasets.

In this work, we present the first geologic map of Imdr Regio, one of the Venus's LTR, and its surrounding areas (Main Map in Supplementary materials). The Imdr Regio Map Area (IRMA) extends between 35°S-50°S in latitude and 195°E-225°E in longitude and covers Imdr Regio and areas that belong to the surrounding plains of Helen, Nsomeka and Wawalag Planitiae (Figures 1 and 2). Imdr Regio was classified as a volcano-dominated igneous rise with a minimum-maximum diameter of 1200–1400 km and a swell height of 1.6 km (Stofan et al., 1995). According to geophysical data and the apparently limited amounts of volcanism, Imdr Regio is thought to be a young topographic rise (Stofan et al., 1995), an idea later reinforced by the discovery of possible recent or even active volcanism in Idunn Mons (D'Incecco et al., 2017; Smrekar et al., 2010), a large volcano that dominates the southeast of the large igneous rise.

CONTACT Iván López ivan.lopez@urjc.es Tecvolrisk Research Group, Departamento de Biología, Geología, Física y Química Inorgánica, Universidad Rey Juan Carlos, 28933. Móstoles, Madrid, Spain

Supplemental map for this article is available online at https://doi.org/10.1080/17445647.2023.2253832.

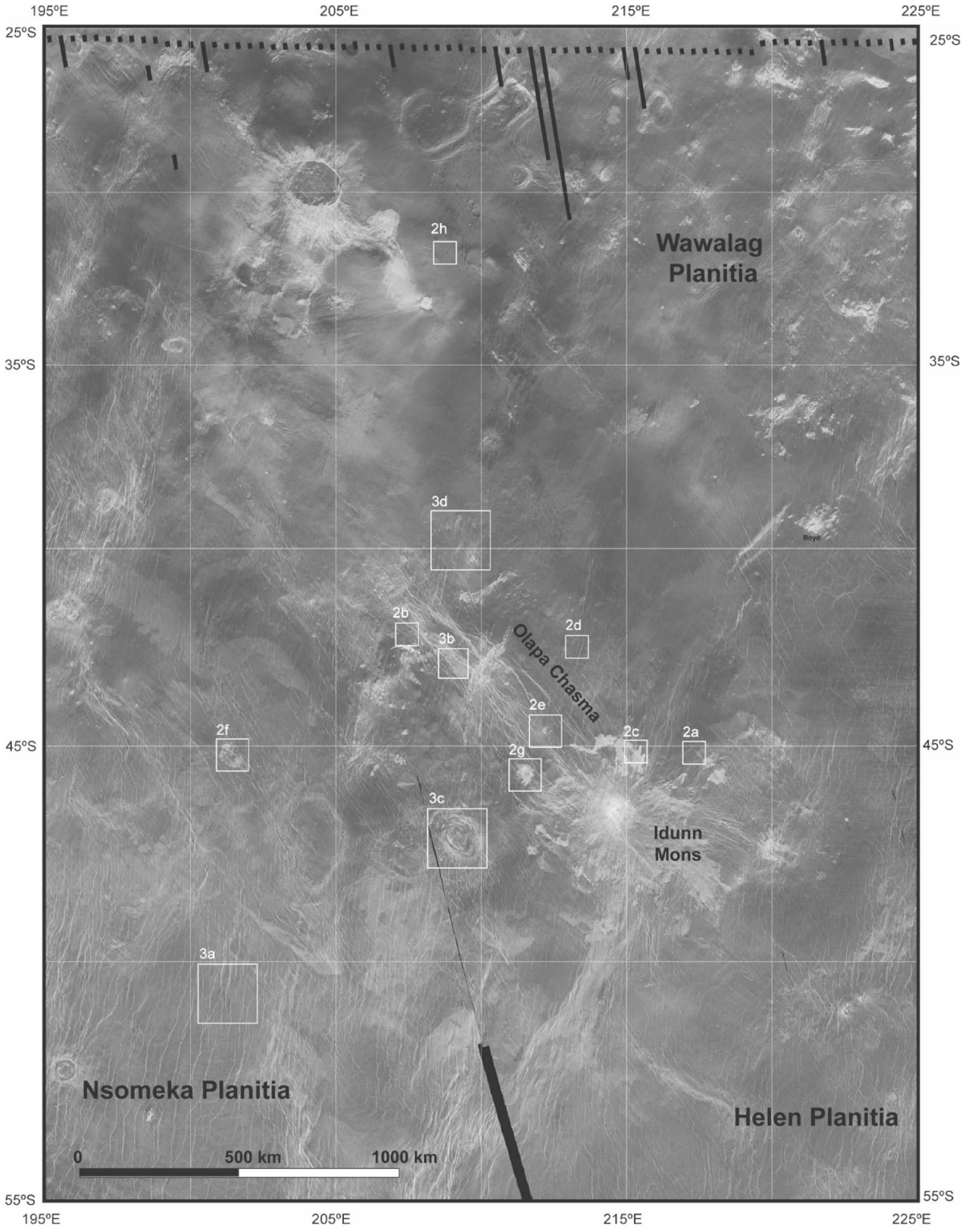

Figure 1. Base map used for the mapping of Imdr Regio. The boxes indicate the location of the examples presented in Figures 3 and 4. Left-looking Magellan SAR mosaic of the map area in Mercator projection.

2. Methods

2.1. Datasets

The high-resolution geologic and tectonic mapping of the Imdr Regio Map Area was carried out using full-resolution NASA Magellan S-band Synthetic Aperture Radar (SAR) imagery with a wavelength of $\lambda = 12$ cm and a frequency of 2.4 GHz and altimetry data. The map area include coverage in both right- and left-illumination full-resolution 'F' (75–100 m/pixel) SAR images, Magellan altimetry (8 km along-track by 20 km across-track footprint with 30-m average

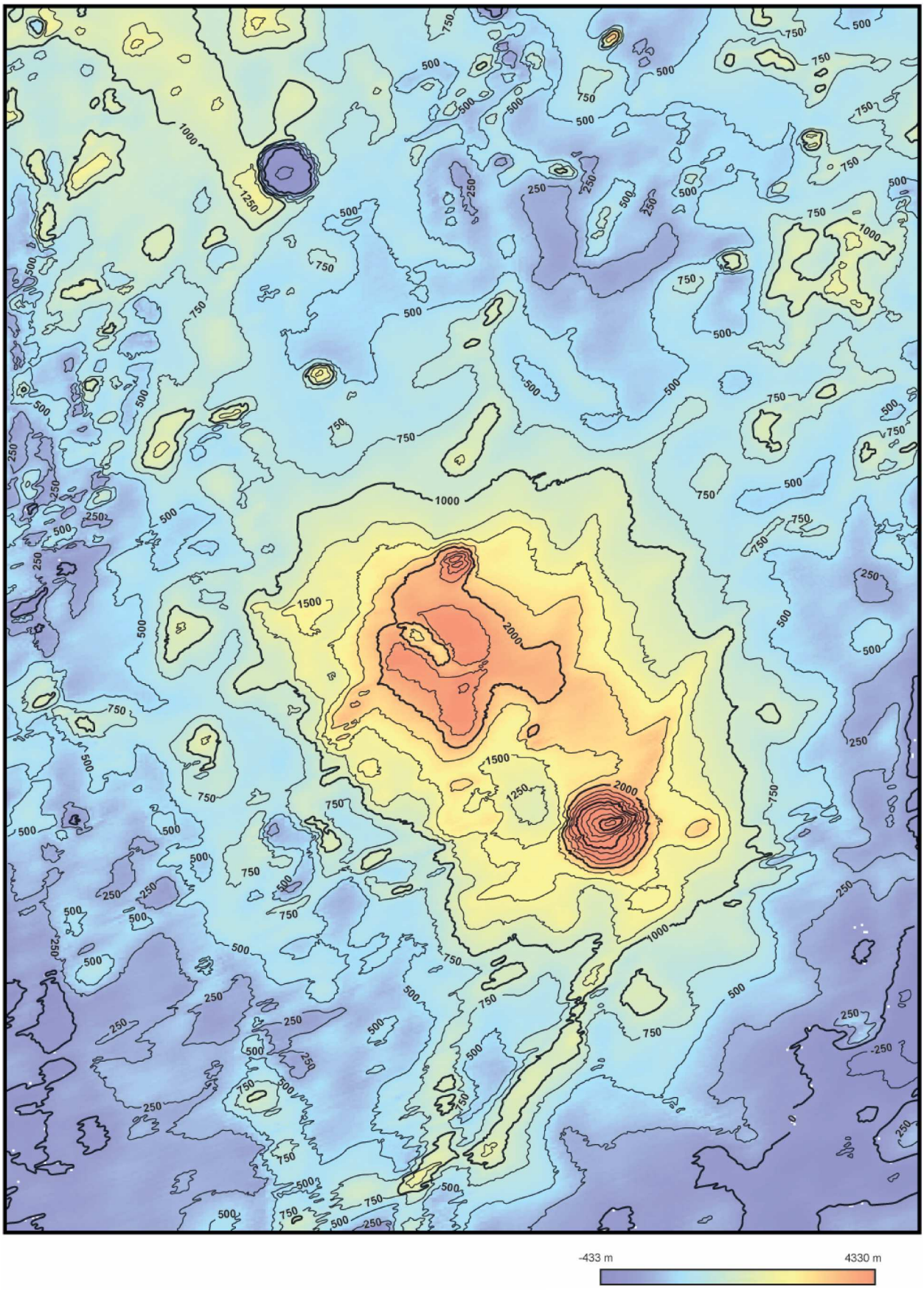

Figure 2. Altimetry of the map area. Contour interval is 250 m. Elevations are referred to the Mean Planetary Radius (6051.84 km). Coordinates, scale, and projection are the same that in Figure 1. Magellan Global Topographic Data Record (GTDR) 4641 m v2.

vertical accuracy which improves to 10 m in smooth areas, Ford et al., 1993) and the rest of available Magellan ancillary data (e.g. Emissivity). All Magellan data were downloaded from the USGS Map-a-Planet website (https://www.mapaplanet.org) in a GIS-ready format for its visualization and analysis. The map and all the data used for mapping is in Mercator projection, better suited to determine direction and structural trends.

2.2. Mapping methodology

The construction of a geologic map is a first step in establishing the geologic history of a region, which in turn provides important information to understand the different processes that may have contributed to the geodynamic evolution of the planet. The methodology that we have used for the definition of geological units and structures is based on standard geological analysis detailed in Wilhelms (1990), and Tanaka et al. (1994) with cautions of Hansen (2000), Zimbelman (2001), Skinner and Tanaka (2003), and McGill and Campbell (2004).

Characteristics of Magellan SAR-data used for geologic mapping and the basics for its interpretation are explored in detail in Ford et al. (1993). The nature of SAR data makes it more straightforward to map lineaments than material units, given their signature as radar reflectors. Lineaments (individual features or families/suites) represent specific geomorphic features (e.g. troughs, ridges) that are going to be interpreted as geologic structures (e.g. fractures, folds, graben, and channels). These geologic structures include primary structures (e.g. those related to the formation or emplacement of the units like volcanic channels or lava flow fronts) and secondary structures (tectonic structures that deform the materials).

After the mapping of tectonic structures, we then proceed to identify different units present in the map area. Primary structures and surface textures, together with radar brightness help to define map units (e.g. mottled, smooth, digitate, and lobate; Ford et al., 1993). However, robust characterization of these surfaces as geologic units, as opposed to geomorphic units, can prove challenging (Brossier et al., 2021; Mouginis-Mark, 2016). This is a result of SAR data being sensitive to surface roughness at the scale of radar wavelength (12.8 cm); rougher surfaces appear bright, smoother surfaces appear dark. It is important to note that such variations are textural and a direct correlation with material type cannot be assumed. This is very important in volcanic settings as materials of similar composition can display different backscatter due to differences in texture of the flows, for example in response to variation of the effusion rate or topography (e.g. pahoehoe vs a'a flows in basaltic materials; Campbell & Rogers, 1994; Rowland & Walker, 1990). In the same way materials of different composition could present similar texture and backscatter values. Another factor to consider is that volcanic materials emplaced on the surface of Venus are the subject of weathering processes that could lead to homogenization on the radar signature that will make difficult to determine surface texture and map to contacts between older materials of similar composition and origin (Arvidson et al., 1992).

Criteria used to distinguish geological units (as opposed to radar units) include the presence of sharp, continuous contacts; truncation of, or interaction with, secondary structures and topography; and presence of primary structures (e.g. flow channels or edifice topography) that allow a reasonable geological interpretation. Some units do not comply to these constraints, limiting their use in the determination of stratigraphic sequences. These units are defined as composite, as they might not be stratigraphically coherent over their entire represented area, and/or they may have been emplaced time transgressively in relation to other units and/or secondary structures.

Older materials like tesserae are pervasively deformed, making it difficult to characterize the original materials. For these units we use the moniker 'terrain', and they are defined by a texture that could imply a shared history.

Mapping of unit contacts is based in limited observable characteristics, so it is hard to follow the contacts along mapped units and we differentiate between (a) definite contacts when distinctive change in the radar properties of the material is observable (i.e. radar contact) and another characteristic can be used for the definition of the unit: clear crosscut relationships, presence of textured materials (e.g. polygonal texture) or interaction with primary and secondary structures; (b) approximate or uncertain contacts when contacts are diffuse due to changes in direction of the contact or homogenization processes; (c) gradational contacts for the mapping of shield-related point-sourced deposits.

Time is an important element in geologic maps, but in the case of Venus a problem in the establishment of temporal relations in regional maps results from the absence of reliable time markers, or marker units. Correlation of map units in planetary maps is typically based on surface impact crater statistics (Schaber et al., 1992). Although this method has some utility for planetary bodies with old surfaces and high crater densities (for example, Moon and Mars), many problems arise on Venus due to crater population characteristics (e.g. Campbell, 1999; Hauck et al., 1998; Izemberg et al., 1994; McKinnon et al., 1997). Fundamentally, Venus' impact craters cannot place any constraints on the age of surface units that cover such small areas as those within the IRMA (e.g. Campbell, 1999; Hauck et al., 1998). This makes the

establishment of relative temporal relationship just possible for those units that are in direct contact or with structures that served as local temporal makers. These temporal constraints are only locally applicable and cannot be robustly extended across the map area, moreover when most of the units are composite in nature. We therefore establish a Sequence of Map Units (SOMU) for the map area that is going to express all the uncertainties that exist regarding temporal relationships, and where temporal relationships between materials that are not in contact are expressed as jagged to indicate the uncertainty (per USGS guidelines; Tanaka et al., 2010).

3. Results

3.1. Structures

The following primary and secondary structures have been identified in the map area and interpretation according to morphology and geologic context is provided.

3.1.1. Primary structures

Channels. Channels represent sinuous to straight low-backscatter features hundreds of kilometers long and a few kilometers wide (Figure 3a); locally they lack apparent topographic relief (Baker et al., 1992; Komatsu et al., 1992). They are more common in the regional plains or associated with large sheet flows. Both the nature of the fluid/lava composition and the formation process (constructive vs erosional) are unknown (e.g. Bussey et al., 1995; Gregg & Greely, 1993; Jones & Pickering, 2003; Lang & Hansen, 2006; Waltham et al., 2008; Williams-Jones et al., 1998).

Pit Chains. Pits or pit chains likely represent regions marked by subsurface excavation and they are interpreted to be the surface expression of dilatational faults or dikes (Figure 3b), implying the transport of magma under the surface (Bleamaster & Hansen, 2001; Ferrill et al., 2004; Okubo & Martel, 1998; Schultz et al., 2004).

Flow fronts. Flow fronts in volcanic materials are sometimes very clear in radar images and help to constrain the maximum extension of volcanic episodes in the eruptive history of a volcanic feature (Figure 3c), direction of the flows and sometimes even the textural character of the material extruded (e.g. Byrnes & Crown, 2002; Mouginis-Mark, 2016; Stofan et al., 2001). Flow fronts together with other primary volcanic structures as channels may constrain the direction and extension of the lava flows, and sometimes help to establish a relative chronology between different flow subunits or flows from different units.

Small volcanoes. Small volcanic edifices (size ≤20 km) are very numerous on the surface of Venus (Figure 3d). Although small volcanic edifices display a broad spectrum of morphologies (e.g. cones, domes, shields; Guest et al., 1992) they are termed generically as shields. Some shields are only discernible by the presence of a pit meanwhile in other cases mounds with a pit are observed. Shields are found isolated in the plains although it is common the occurrence of groups of edifices forming clusters or *shield fields* (*colles*), sometimes associated with large tectonomagmatic features (e.g. coronae and large volcanic edifices).

Intermediate volcanoes. Volcanic edifices of intermediate size (size ≥ 20 km ≤ 100 km) are also common on the surface of Venus (Figure 3e). There are volcanic features particular of this size: steep-sided or pancake domes and stellate domes (Crumpler et al., 1997). Another characteristic commonly observable in edifices of these size and morphology is the presence of lateral flank collapses and related deposits (Figure 3f). Sometimes we can only observe the scarp associated to the volcano flank collapse because the associated deposits are covered by younger material (López, 2011).

Crater rims. Impact cratering is a process described across the solar system. A crater is characterized, from the morphological point of view, by a raised rim surrounding a topographic low with sometimes a central peak (Figure 3g). In craters, we map the rims as primary structures and the ejecta blanket, rough and blocky material around the crater expelled by the impact, as a map unit.

Surficial deposits. The northern half of the map area is characterized by the presence of surficial deposits like crater haloes associated to Isabella and Cohn craters. These materials are composed of fine dust that covers the different units and structures but still allowing their observation. The extent of the individual crater haloes is difficult to constrain as most of the northern map area is affected by the presence of these deposits. The presence of these surficial deposits also makes difficult the determination of the contacts between units that are covered by them. Locally these surficial deposits are remobilized by wind (Figure 3h), forming eolian features oriented to west-southwest, coherent with direction of wind-related crater features in the planet (Campbell et al., 1992).

Hummocky terrains: Deposits associated with the collapse of volcanic edifices, known as hummocky terrains (e.g. Siebert, 1984) display bright appearance and blocky texture in radar images (Figure 3f).

Contacts. We have determined three types of contacts: (a) clear or definite contacts for those contacts the present distinctive changes in the radar properties, and/or another characteristic can be used for the definition of the unit (e.g. interaction with secondary structures); (b) approximate or uncertain contacts when contacts are diffuse due to changes in direction of the contact, homogenization and lack of other

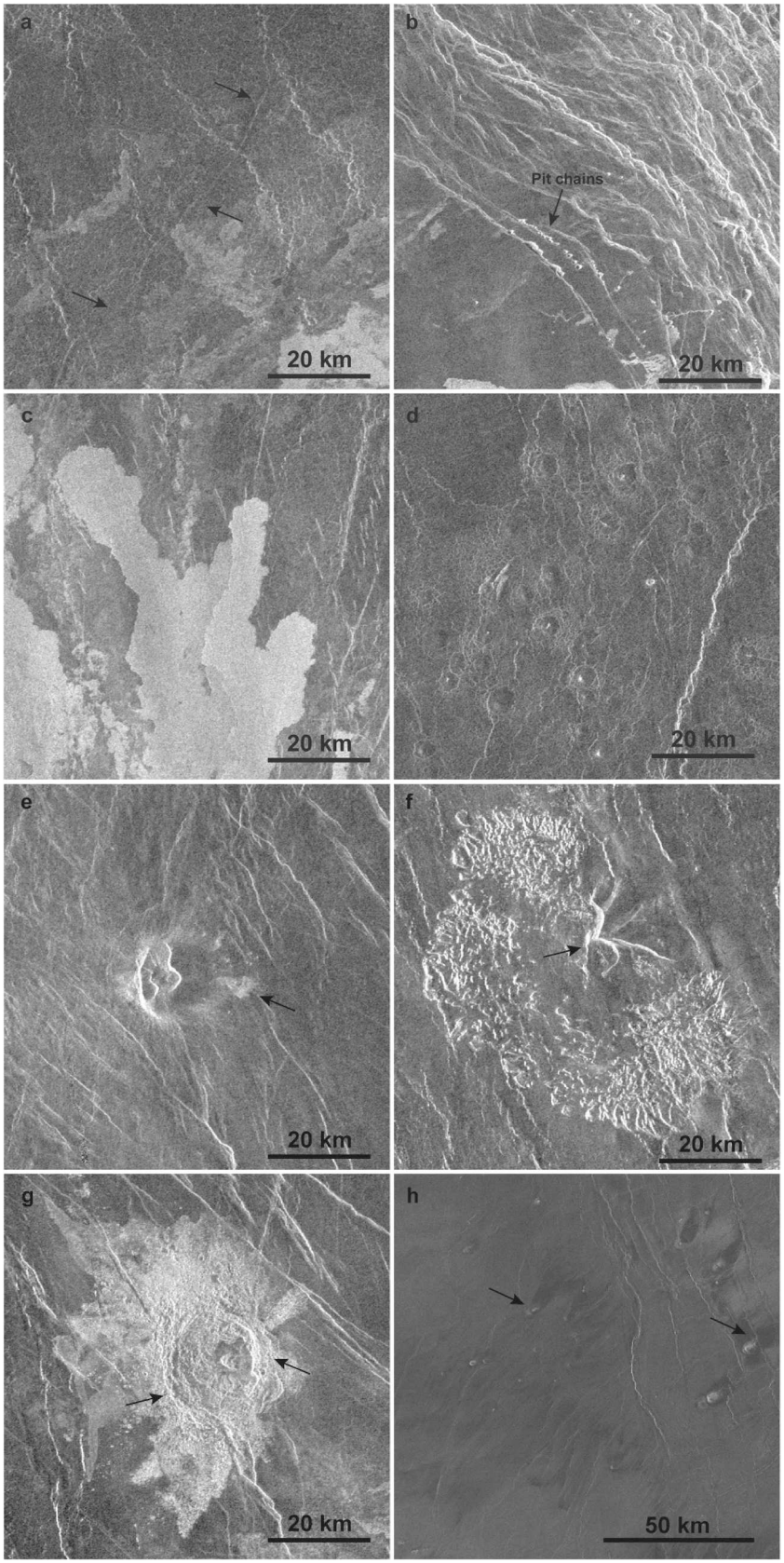

Figure 3. Examples of primary structures in the map area. (a) Channel in the sheet flows of Idunn Mons (arrows indicate the trace of the channel); (b) Pit chains in Olapa Chasma (arrow indicate a chain of pits with associated volcanic materials flowing to the SE); (c Flows fronts in Idunn Mons. The bright flows overlap indicating different effusive event in the volcano history; (d) small volcanoes in the volcanic plains; (e) Zana Tholus, an intermediate volcano in Imdr Regio. The flanks of the volcano are embayed by flows from near sources. The arrow indicated the presence of small debris avalanche of lava flow in the lower eastern flank; (f) Hummocky terrain. This type of deposit indicates the presence of lateral flank collapse processes in volcanoes. The arrow marks the scarps that mark the collapse structure deposit and the remains of the original edifice; (g) Sandel crater. Example of an impact crater with a clear rim and central peak; (h) Surficial deposits. Dust produced by impacts in the volcanic plains. The arrows mark the presence of wind streaks associated with small volcanoes. All the images are left-looking Magellan SAR images in normal mode.

characteristics that could help to define the contact and; (c) gradational contacts for the mapping of shield-related point-sourced deposits.

3.1.2. Secondary structures

Contractional structures. Ridges and wrinkle ridges (Figure 4a) are linear structures of positive relief interpreted as the surface expression of thrust faults and/or folds (Schultz, 2000). Wrinkle ridges are long, narrow, sinuous features with varying width that occur in parallel sets with constant spacing over great distances (Banerdt et al., 1997). In the map area, almost all units except for basement materials and the most recent volcanic units are deformed by wrinkle ridges. Locally, suites of wrinkle ridges seem to be formed in response to late structural reactivation or inversion (e.g. DeShon et al., 2000). The principal trend in the map area is the *180° trend*, that together with the *Helen Planitia trend* dominate in this part of the planet (Billoti & Suppe, 1999).

Extensional structures. Under the generic term fractures, we consider linear structures of extensional origin. They could be simple fractures or troughs interpreted as graben (Figure 4b), but sometimes these structures are at the limit of the image resolution and structures mapped as fractures could indeed be troughs. Simple fractures are visible as just simple radar-bright lineaments. In these structures, radar brightness is not related to the orientation of the structure respecting the radar-look direction, as the lineament is seen with the same characteristics both in left-looking and right-looking images. This is consistent with an open fracture, joint-like interpretation for this type of structures (Banerdt et al., 1997). Troughs are paired sets of lineaments interpreted in most of the cases as graben.

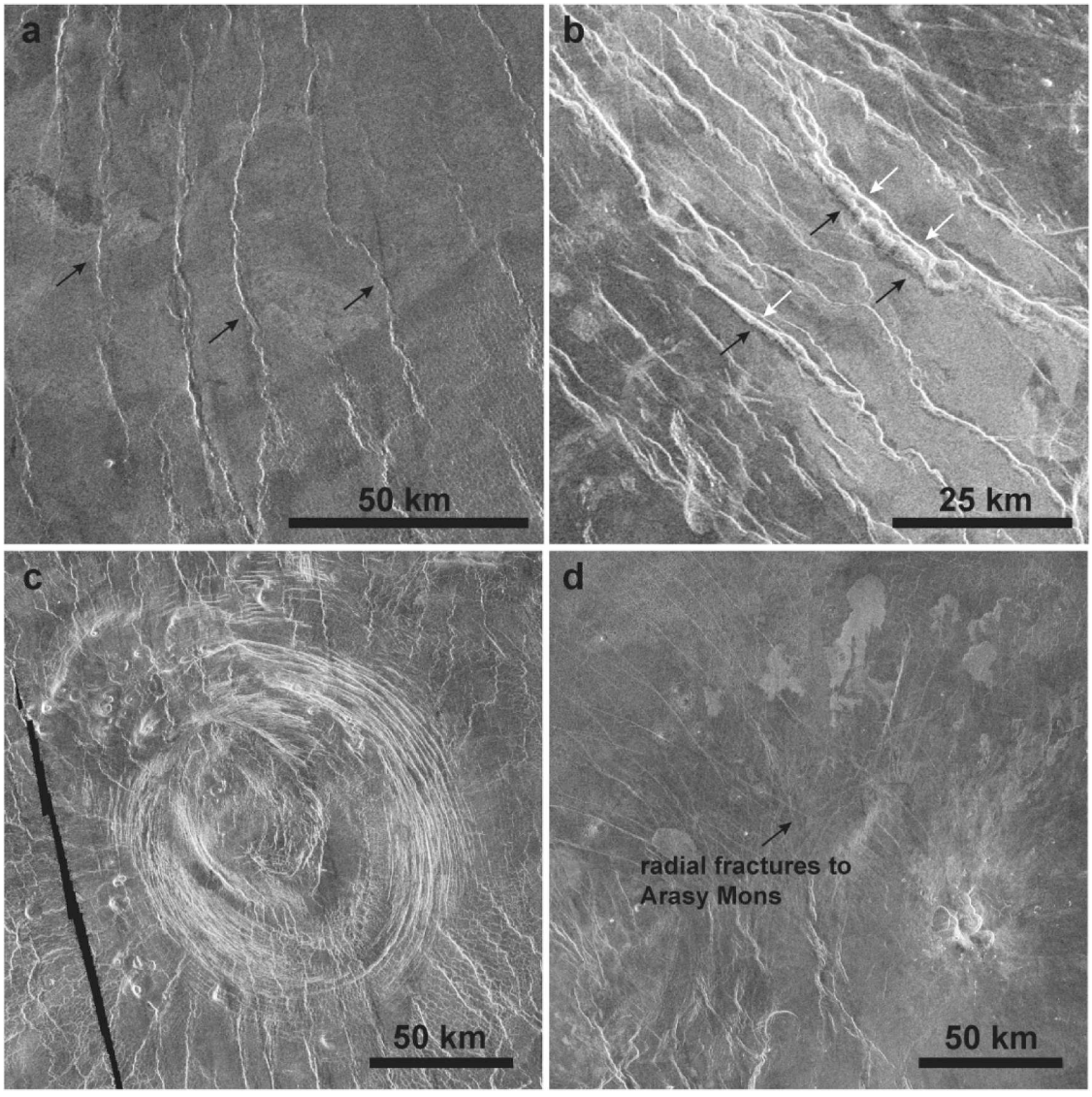

Figure 4. Examples of secondary structures in the map area. (a) wrinkle ridges (b) Fractures and graben in Olapa Chasma. Black arrows indicate the face of the graben oriented away from the radar illumination that generate a shadow. White arrows indicate the face of the graben oriented toward the radar illumination that generate a bright surface; (c) Local concentric fractures in Boann Corona; (d) Local radial fractures to Arasy Mons. All the images are left-looking Magellan SAR images in normal mode.

We have mapped different families or suites of fractures and graben based on their regional or local nature. Regional fractures are those that extend across the map area and that are interpreted of regional origin. Different families of regional fractures and graben with different trends are found deforming regional plains and basal plain materials. The most important and widely distributed of these older regional fracture suites is a NE-SW trending suite that is present in different parts of the map area deforming materials of the basement and the basal plain materials. In the IRMA, NW-SE trending fractures and graben of Olapa Chasma are the principal structural suite, cutting the different materials formed throughout the evolution of the large topographic rise. They are locally associated to pit chains, situation that suggest that some of these fractures and graben can be related to the emplacement of underlying dikes.

We have also mapped different suites of local fractures and graben associated to tectono-magmatic structures as coronae, novae and large volcanoes. These local suites of fractures can be concentric (Figure 4c) or radial (Figure 4d) to the tectonomagmatic feature and are result of local stress fields associated to their formation and evolution (Grindrod et al., 2005; Stofan et al., 1992).

3.2. Map units

Tessera terrain, undivided (tu). Isolated outcrops of high-backscatter and relatively high relief materials. Extensively deformed by suites of local and regional structures. Individual outcrops display different structural assemblages and deformational histories.

Lower plain materials, undivided (lpmu). High- to low-radar-backscatter volcanic materials, can include shields (generally less than 5 km diameter). Composite unit that marks a local older terrain embayed by regional plains and volcanic materials. Extensively deformed by regional wrinkle ridges, regional fractures and suites of local radial and concentric structures related to the evolution of volcano-tectonic structures.

Smooth plains, undivided (spu). Low-to-high backscatter material with smooth texture. Composite unit that forms the regional plains. In some locations the presence of mantling materials (crater haloes) makes difficult to determine texture and backscatter. Internally discontinuous flow boundaries and volcanic primary structures that include channels and shields (locally clustered) suggest a volcanic origin. Extensively deformed by regional wrinkle ridges, regional fractures and suites of local radial and concentric structures related to the evolution of volcano-tectonic structures. The composite nature of this unit precludes its use as a marker unit across the map area and only local temporal relations can be determined.

Textured plains, undivided (tpu). Low- to high backscatter material with a reticulate/polygonal texture. This texture varies in the size of with polygons that in some locations are in the limits of the image resolution. Composite unit that can be part of the regional plains but also of the early volcanic activity in Imdr Regio. In some locations the presence of mantling materials (crater haloes) makes difficult to determine texture and backscatter and the contact with surrounding materials. Internally heterogeneous, primary structures include channels and shields (locally clustered) that suggest a volcanic origin. In some locations texture is related to the presence of shield clusters and could be genetically related. Extensively deformed by regional wrinkle ridges, regional fractures and suites of local radial and concentric structures related to the evolution of volcano-tectonic structures. The composite nature of this unit precludes its use as a marker unit across the map area and only local temporal relations can be determined.

Crater material, undivided (cu). High backscatter and blocky texture. Includes ejecta blankets, crater floor and central peaks. The composite nature of this unit precludes its use as a marker unit across the map area and only local temporal relations of the crater materials with other units and structures can be determined.

Crater flow material, undivided (cfu). High backscatter flow materials associated with impact craters. Lobate flows and flow structures allow to determine flow direction. The composite nature of this unit precludes its use as a marker unit across the map area and only local temporal relations of the crater materials with other units and structures can be determined.

Flows from Kupo Patera (fpK). Intermediate-to-high backscatter materials associated with Kupo Patera (41.9°S/195.5°E) and other near volcano-tectonic features. Proximal flows to Kupo Patera display high backscatter and clear flow lobes. Intermediate-size volcanoes around Kupo Patera could also contribute to the unit. Deformed by regional wrinkle ridges. Relation to regional fractures and concentric structures related to the formation and evolution of Kupo Patera is time transgressive.

Flows from Arasy Mons (fmA). Intermediate backscatter and mottled texture. Composite unit made of overlapping volcanic flows related to Arasy Mons (40.2°S/209.7°E). Clear lobate flows allow to trace the direction and extent if the volcanic flows to the N and NW of the volcano. Secondary pits and small volcanoes on the flanks also could contribute to the unit. A radial fracture system associated with the formation of the volcano cuts, but is also partially covered by, the materials of the unit. Locally cut by fractures and graben of Olapa Chasma.

Flows from Firtos Mons (fmF). Intermediate backscatter materials around Firtos Mons (47.3°S/220°E).

A radial fracture system associated with Firtos Mons cuts, but is also partially covered by, the materials of the unit. Lack of clear flow lobes makes difficult to clearly delineate the limits of the unit. Embayed volcanic features and clusters of small volcanoes could have also contribute to the unit. Deformed by regional wrinkle ridges.

Flows from Ignirtoq Tholi (ftI). Intermediate to high backscatter and mottled texture. Composite unit made of overlapping volcanic flows related to Ignirtoq Tholi (50.9°S/222.8°E). Clear lobate flows allow to locally trace the direction and extent if the volcanic flows. Flows postdate radial fractures associated to Ignirtoq Tholi but are deformed by regional wrinkle ridges.

Flows from unnamed paterae (fpu). Intermediate to high backscatter flows associated with a group of small unnamed paterae. Relation to concentric structures related to the formation of the different patera and regional wrinkle ridges is time transgressive.

Shield field and associated materials near Payne-Gaposchkin Patera (sfPG). Low to intermediate backscatter materials formed by clusters of individual < 10 km kilometer-diameter edifices and associated flows. Gradational contacts with surrounding units due to the point-source nature of shield volcanism. Locally deformed by regional wrinkle ridges, regional fractures and suites of local radial and concentric structures related to the evolution of volcano-tectonic structures.

Shield field and associated materials in eastern Wawalag Planitia (sfW). Low to intermediate backscatter materials formed by clusters of individual < 10 km kilometer-diameter edifices and associated flows. Gradational contacts with surrounding units due to the point-source nature of shield volcanism. Locally deformed by regional wrinkle ridges, regional fractures and suites of local radial and concentric structures related to the evolution of volcano-tectonic structures.

Shield field and associated materials in northern Olapa Chasma (sfNO). Low to intermediate backscatter materials formed by clusters of individual < 10 km kilometer-diameter edifices and associated flows. Gradational contacts with surrounding units due to the point-source nature of shield volcanism. Locally deformed by regional wrinkle ridges, regional fractures and suites of local radial and concentric structures related to the evolution of volcano-tectonic structures.

Shield field and associated materials in western Olapa Chasma (sfWO). Intermediate backscatter materials with mottle to reticulate textures. Associated to intermediate volcanoes and clusters of small volcanoes in western Olapa Chasma. Locally flow lobes allow to trace the extent and direction of the flows. Materials of this unit are locally cut by local NW- and NE-trending regional fractures that are also locally postdated by materials of the unit. Deformed by regional wrinkle ridges.

Shield field and associated materials in eastern Olapa Chasma (sfEO). Intermediate to low backscatter and smooth texture. Some small flows can be traced to small volcanoes, but the source of some unit materials is not clear. Locally deformed by local radial fractures of Idunn Mons and some wrinkle ridges but is general the materials of the unit lack significant deformation.

Flows from Olapa Chasma (fchO). Low to high backscatter materials with textures that variate from smooth to locally mottled appearance. Clear flow lobes allow to determine extent and direction of flows. This unit is a composite unit formed by flows that originate in fractures and graben of Olapa Chasma, but also locally can be related to individual shields and shield clusters. Different flows that form this unit include Robigo, Saosis and Nyakaya flucti. Materials of this unit are contemporaneous with the formation of Olapa Chasma, with volcanic materials postdating and being deformed by individual structures of the rift system. Locally deformed by radial fractures of Idunn and Arasy montes, and, but very locally by regional fractures and wrinkle ridges. It is a composite unit that only allows for the determination of local temporal relationships.

Flows from Idunn Mons, member 1 (fmI1). Low backscatter and mostly homogenous sheet flows that locally exhibit a mottled texture in their terminal areas. The presence of a large channel suggest that these large flows could be channel-fed, but also could correspond to a section of the flow that was channelized or a channel that fed later flows units. Extensively deformed by regional wrinkle ridges, fractures, and graben of Olapa Chasma, and local radial fractures of Idunn Mons. Locally materials of the unit cover these radial fractures, indicating that they could be contemporaneous and that the volcanic flows could be genetically related to the radial fractures.

Flows from Idunn Mons, member 2 (fmI2). Intermediate backscatter overlapping digitate flows with local bright edges and hummocky texture. Locally deformed by wrinkle ridges, especially in their distal areas. Contemporaneous with local radial fractures of Idunn Mons and fractures and graben of Olapa Chasma.

Flows from Idunn Mons, member 3 (fmI3). High backscatter overlapping digitate flows that present an internal homogeneous structure. Some of the flows are channelized. Contemporaneous with the local radial fractures of Idunn Mons and with fractures and graben of Olapa Chasma.

Flows from Idunn Mons, member 4 (fmI4). Intermediate-to-high backscatter multiple overlapping digitate flows that radiate from the central summit.

Contemporaneous with the local radial fractures of Idunn Mons and with fractures and graben of Olapa Chasma. Some flows whose source cannot be traced to the summit could be related to fracture-fed flows in the flanks and related to the rift fractures.

Flows from Idunn Mons, member 5 (fmI5). Intermediate-to-high backscatter multiple overlapping digitate flows that form the upper volcano flanks. Some of the flows near the summit present narrow length-to-width ratios. Flows of this unit are contemporaneous with fractures and graben of Olapa Chasma but seem to postdate the local radial fractures of Idunn Mons. Some flows could be fracture-fed flows originated in fractures and graben of Olapa Chasma.

4. Conclusions

This study represents the first detailed geological map of the Imdr Regio of Venus. In the map area, the regional plains are composed of local outcrops of tesserae and other local materials that are postdated by the large regional plains (Smooth and Textured plains undivided). These materials are deformed by regional fractures, wrinkle ridges of the 180° and Helen Planitia regional trends (Billoti & Suppe, 1999), and by local fracture suites related to the formation of coronae and other large tectonomagmatic features. Imdr Regio is dominated by the NW-SE trending Olapa Chasma with local fractures and graben associated to the formation of large volcanoes and other tectonomagmatic units. Units in Imdr Regio are related to the formation of large volcanoes like Idunn Mons and to the magmatism associated to the Olapa Chasma rift system. Other units include clusters of small shields and associated materials that formed throughout the history of Imdr Regio. Throughout the map area several units were formed by crater ejecta materials and local flows associated to impact craters (e.g. Isabella and Boyd). In the northern half of the map area surficial materials (i.e. dust) associated to the impact processes cover the different structures and units. The geologic mapping has revealed a complex tectono-magmatic history in the region, with different units related to different types of structures and magmatic styles.

Software

Data visualization, analysis, and interpretation were carried out using ArcGIS 10.4™ and geologic mapping was conducted using Adobe Illustrator 27.7™.

Disclosure statement

No potential conflict of interest was reported by the author(s).

Funding

This research was partially supported by Italian Space Agency (ASI/2020-15-HH.0 and ASI/2022-15-HH.0 agreements).

Data availability statement

All the data used for this research was obtained by the NASA Magellan mission and can be publicly accessed through the Map a Planet (MAP) cloud processing tool from the USGS Astrogeology Science Center (https://astrogeology.usgs.gov/search/results?q=MAP2&k1=target&v1=Venus).

References

Arvidson, R. E., Greeley, R., Malin, M. C., Saunders, R. S., Izenberg, N., Plaut, J. J., Stofan, E. R., & Shepard, M. K. (1992). Surface modification of Venus as inferred from magellan observation of plains. *Journal of Geophysical Research*, *97*(E8), 13303–13317. https://doi.org/10.1029/92JE01384

Baker, V. R., Komatsu, G., Parker, T. J., Gulick, V. C., Kargel, J. S., & Lewis, J. S. (1992). Channels and valleys on Venus: Preliminary analysis of Magellan data. *Journal of Geophysical Research: Planets*, *97*(E8), 13421–13444. https://doi.org/10.1029/92JE00927

Banerdt, W. B., McGill, G. E., & Zuber, M. T. (1997). Plains tectonism on Venus. In S. W. Bougher, D. M. Hunten, & R. J. Phillips (Eds.), *Venus II: Geology, geophysics, atmosphere, and solar environment* (pp. 901–930). University of Arizona Press.

Billoti, F., & Suppe, J. (1999). The global distribution of wrinkle ridges on Venus. *Icarus*, *139*(1), 137–159. https://doi.org/10.1006/icar.1999.6092

Bleamaster, L. F., & Hansen, V. L. (2001). The Kuanja/Vir-Ava Chasmata: A coherent intrusive complex on Venus. *In Lunar and Planetary Science Conference XXXII*, Abstract #1316, Lunar and Planetary Institute, Houston (CD-ROM).

Brossier, J., Gilmore, M. S., Toner, K., & Stein, A. J. (2021). Distinct mineralogy and age of individual lava flows in Atla Regio, Venus derived from Magellan radar emissivity. JGR 126, e2020JE006722. https://doi.org/10.1029/2020JE006722

Bussey, D. B. J., Sorenson, S. A., & Guest, J. E. (1995). Factors influencing the capability of lava to erode its substrate: Application to Venus. *Journal of Geophysical Research: Planets*, *100*(E8), 16941–16948. https://doi.org/10.1029/95JE00894

Byrnes, J. M., & Crown, D. A. (2002). Morphology, stratigraphy and surface roughness properties of Venusian lava flow fields. *Journal of Geophysical Research: Planets*, *107*(E10), 5079. https://doi.org/10.1029/2001JE001828

Campbell, B. A. (1999). Surface formation rates and impact crater densities on Venus. *Journal of Geophysical Research: Planets*, *104*(E9), 21951–21955. https://doi.org/10.1029/1998JE000607

Campbell, B. A., & Rogers, P. G. (1994). Bell Regio, Venus: Integration of remote sensing data and terrestrial analogs for geologic analysis. *Journal of Geophysical Research: Planets*, *99*(E10), 21153–21171. https://doi.org/10.1029/94JE01862

Campbell, D. B., Stacy, N. J. S., Newman, W. I., Arvidson, R. E., Jones, E. M., Musser, G. S., Roper, A. Y., & Schaller, C.

(1992). Magellan observations of extended impact crater related features on the surface of Venus. *Journal of Geophysical Research: Planets*, *97*(E10), 16249–16277. https://doi.org/10.1029/92JE01634

Crumpler, L. S., Aubele, J. C., Senske, D. A., Keddie, S. T., Magee, K. P., & Head, J. W. (1997). Volcanoes and centers of volcanism on Venus. In S. W. Bougher, D. M. Hunten, & R. J. Phillips (Eds.), *Venus II: Geology, geophysics, atmosphere, and solar environment* (pp. 697–756). University of Arizona Press.

DeShon, H. R., Young, D. A., & Hansen, V. L. (2000). Geologic evolution of southern Rusalka Planitia. *Venus. Journal of Geophysical Research:Planets*, *105*(E3), 6983–6995. https://doi.org/10.1029/1999JE001155

D'Incecco, P., Filiberto, J., López, I., Gorinov, D., Komatsu, G., Martynov, A., & Pisarenko, P. (2021). The young volcanic rises on Venus: A key scientific target for future orbital and in-situ measurements on Venus. *Solar System Research*, *55*(4), 315–323. https://doi.org/10.1134/S0038094621040031

D'Incecco, P., Müller, N., Helbert, J., & D'Amore, M. (2017). Idunn Mons on Venus: Location and extent of recently active lava flows. *Planet. Space Sci*, *136*, 25–33. https://doi.org/10.1016/j.pss.2016.12.002

Ferrill, D. A., Wyrick, D. Y., Morris, A. P., Sims, D. W., & Franklin, N. M. (2004). Dilational fault slip and pit chain formation on Mars. *GSA Today*, *14*(*10*), 4–12. https://doi.org/10.1130/1052-5173(2004)014<4:DFSAPC>2.0.CO;2

Ford, J. P., Plaut, J. J., Weitz, C. M., Farr, T. G., Senske, D. A., Stofan, E. R., Michaels, G., & Parker, T. J. (1993). *Guide to Magellan image interpretation* (pp. 93–24) JPL Publication.

Gregg, T. K. P., & Greely, R. (1993). Formation of venusian canali: Considerations of lava types and their thermal behaviors. *Journal of Geophysical Research: Planets*, *98* (E6), 10873–10882. https://doi.org/10.1029/93JE00692

Grindrod, P. M., Nimmo, F., Stofan, E. R., & Guest, J. E. (2005). Strain at radially fractured centers on Venus. *Journal of Geophysical Research: Planets*, *110*(E12), E12002. https://doi.org/10.1029/2005JE002416

Guest, J. E., Bulmer, M. H., Aubele, J. C., Beratan, K., Greely, R., Head, J. W., Micheals, G., Weitz, C., & Wiles, C. (1992). Small volcanic edifices and volcanism in the plains of Venus. *Journal of Geophysical Research: Planets*, *97*(E10), 15949–15966. https://doi.org/10.1029/92JE01438

Hansen, V. L. (2000). Geologic mapping of tectonic planets. *Earth and Planetary Science Letters*, *176*(3-4), 527–542. https://doi.org/10.1016/S0012-821X(00)00017-0

Hauck, S. A., Phillips, R. J., & Price, M. H. (1998). Venus: Crater distribution and plains resurfacing models. *Journal of Geophysical Research-Planets*, *103*(E6), 13635–13642. https://doi.org/10.1029/98JE00400

Head, J. W., Crumpler, L. S., Aubele, J. C., Guest, J. E., & Saunders, R. S. (1992). Venus volcanism: Classification of volcanic features and structures, associations, and global distribution from Magellan data. *Journal of Geophysical Research: Planets*, *97*(E8), 13153–13197. https://doi.org/10.1029/92JE01273

Herrick, R. R., & Hensley, S. (2023). Surface changes observed on a venusian volcano during the Magellan mission. *Science*, *379*(6638), 1205–1208. https://doi.org/10.1126/science.abm7735

Izemberg, N. R., Arvidson, R. E., & Phillips, R. J. (1994). Impact crater degradation on venusian plains. *Geophysical Research Letters*, *21*(4), 289–292. https://doi.org/10.1029/94GL00080

Jones, A. P., & Pickering, K. T. (2003). Evidence for aqueous fluid-sediment transport and erosional processes on Venus. *Journal Geological Society of London*, *160*(2), 319–327. https://doi.org/10.1144/0016-764902-111

Komatsu, G., Kargel, J. S., & Baker, V. R. (1992). Canali-type channels on Venus: Some genetic constraints. *Geophysical Research Letters*, *19*(13), 1415–1418. https://doi.org/10.1029/92GL01047

Lang, N. P., & Hansen, V. L. (2006). Venusian channel formation as a subsurface process. *Journal of Geophysical Research: Planets*, *111*(E4), E04001. https://doi.org/10.1029/2005JE002629

López, I. (2011). Embayed intermediate volcanoes on Venus: Implications for the evolution of the volcanic plains. *Icarus*, *213*(1), 73–85. https://doi.org/10.1016/j.icarus.2011.02.022

McGill, G. E., & Campbell, B. A. (2004). Ages of Venusian ridge belts relative to regional plains: *Lunar and Planetary Science Conference XXXVI*, Houston, Tex., abstract 1143 [CD ROM].

McKinnon, W. B., Zahnle, K. J., Ivanov, B. A., & Melosh, H. J. (1997). Cratering on Venus: Models and observations. In S. W. Bougher, D. M. Hunten, & R. J. Phillips (Eds.), *Venus II: Geology, geophysics, atmosphere, and solar environment* (pp. 931–965). University of Arizona Press.

Mouginis-Mark, P. J. (2016). Geomorphology and volcanology of Maat Mons, Venus. *Icarus*, *277*, 433–441. https://doi.org/10.1016/j.icarus.2016.05.022

Okubo, C. H., & Martel, S. J. (1998). Pit crater formation on Kilauea volcano, Hawaii. *Journal of Volcanology and Geothermal Research*, *86*(1-4), 1–18. https://doi.org/10.1016/S0377-0273(98)00070-5

Phillips, R. J., & Hansen, V. L. (1994). Tectonic and magmatic evolution of Venus. *Annual Review of Earth and Planetary Sciences*, *22*(1), 597–654. https://doi.org/10.1146/annurev.ea.22.050194.003121

Rowland, S. K., & Walker, G. P. L. (1990). Pahoehoe and a'a in Hawaii: Volumetric flow rate controls the lava structure. *Bulletin of Volcanology*, *52*(8), 615–628. https://doi.org/10.1007/BF00301212

Schaber, G. G., Strom, R. G., Moore, H. J., Soderblom, L. A., Kirk, R. L., Chadwick, D. J., Dawson, D. D., Gaddis, L. R., Boyce, J. M., & Russell, J. (1992). Geology and distribution of impact craters on Venus: What are they telling us? *Journal of Geophysical Research*, *97*(E8), 13257–13301. https://doi.org/10.1029/92JE01246

Schultz, R. A. (2000). Localization of bedding plane slip and backthrust faults above blind thrust faults: Keys to wrinkle ridge structure. *Journal of Geophysical Research*, *105* (E5), 12035–12052. https://doi.org/10.1029/1999JE001212

Schultz, R. A., Okubo, C. H., Goudy, C. L., & Wilkins, S. J. (2004). Igneous dikes on Mars revealed by Mars Orbiter Laser Altimeter topography. *Geology*, *32*(10), 889–892. https://doi.org/10.1130/G20548.1

Siebert, L. (1984). Large volcanic debris avalanches: Characteristics of the source areas, deposits, and associated eruptions. *Journal of Volcanology and Geothermal Research*, *22*(3-4), 163–197. https://doi.org/10.1016/0377-0273(84)90002-7

Skinner, J. A., & Tanaka, K. L. (2003). How should map units be defined? *Lunar and Planetary Science Conference XXXIV*, Houston, Tex., abstract 2100 [PDF].

Smrekar, S., Stofan, E. R., Mueller, N., Treiman, A., Elkins-Tanton, L., Helbert, J., Piccioni, G., & Drossart, P. (2010). Recent hotspot volcanism on Venus from VIRTIS emissivity data. *Science*, *328*(5978), 605–608. https://doi.org/10.1126/science.1186785

Smrekar, S. E., Kiefer, W. S., & Stofan, E. R. (1997). Large volcanic rises on Venus. In S. W. Bougher, D. M. Hunten, & R. J. Phillips (Eds.), *Venus II: Geology, geophysics, atmosphere, and solar environment* (pp. 845–878). University of Arizona Press.

Solomon, S. C., Smrekar, S. E., Bindschadler, D. L., Grimm, R. E., Kaula, W. M., McGill, G. E., Phillips, R. J., Saunders, R. S., Schubert, G., Squyres, S. W., & Stofan, E. R. (1992). Venus tectonics: An overview of Magellan observations. *Journal of Geophysical Research: Planets*, *97*(E8), 13199–13255. https://doi.org/10.1029/92JE01418

Stofan, E. R., Guest, J. E., & Copp, D. L. (2001). Development of large volcanoes on Venus: Constraints from Sif, Gula, and Kunapipi Montes. *Icarus*, *152*(1), 75–95. https://doi.org/10.1006/icar.2001.6633

Stofan, E. R., Sharpton, V. L., Schubert, G., Baer, G., Bindschadler, D. L., Janes, D. M., & Squyres, S. W. (1992). Global distribution and characteristics of coronae and related features on Venus: Implications for origin and relation to mantle processes. *Journal of Geophysical Research Planets*, *97*(E8), 13347–13378. https://doi.org/10.1029/92JE01314

Stofan, E. R., Smrekar, S. E., Bindschadler, D. L., & Senske, D. A. (1995). Large topographic rises on Venus: Implications for mantle upwelling. *Journal of Geophysical Research: Planets*, *100*(*E11*), 23317–23327. https://doi.org/10.1029/95JE01834

Tanaka, K. L., Anderson, R., Dohm, J. M., Hansen, V. L., McGill, G. E., & Pappalardo, R. T. (2010). Planetary structural mapping. In T. R. Watters, & R. A. Schultz (Eds.), *Planetary tectonics* (pp. 349–394). Cambridge University Press.

Tanaka, K. T., Moore, H. J., Schaber, G. G., Chapman, M. G., Stofan, E. R., Campbell, D. B., Davis, P. A., Guest, J. E., McGill, G. E., Rogers, P. G., Saunders, R. S., & Zimbelman, J. R. (1994). The Venus geologic mapper's handbook. *USGS, Open-File Report 94-438*.

Waltham, D., Pickering, K. T., & Bray, V. J. (2008). Particulate gravity currents on Venus. *Journal of Geophysical Research-Planets*, *113*(E2), E02012. https://doi.org/10.1029/2007JE002913

Wilhelms, D. E. (1990). Geologic mapping. In R. Greely, & R. M. Batson (Eds.), *Planetary mapping* (pp. 208–259). Cambridge University Press.

Williams-Jones, G., Williams-Jones, A. E., & Stix, J. (1998). The nature and origin of Venusian canali. *Journal of Geophysical Research: Planets*, *103*(E4), 8545–8555. https://doi.org/10.1029/98JE00243

Zimbelman, J. R. (2001). Image resolution and evaluation of genetic hypotheses for planetary landscapes. *Geomorphology*, *37*(3-4), 179–199. https://doi.org/10.1016/S0169-555X(00)00082-9